Oxidation chemistry of adenine N^1-oxide, a potent oncogenic agent, at a pyrolytic graphite electrode

Rajendra N. Goyal * and Aditi Sangal

Department of Chemistry, I. I. T. Roorkee, Roorkee, 247667, India.
E-mail: rngcyfcy@iitr.ernet.in

Received (in Cambridge, UK) 30th April 2002, Accepted 6th August 2002
First published as an Advance Article on the web 26th September 2002

The electrochemical oxidation of adenine N^1-oxide has been studied at a pyrolytic graphite electrode in phosphate buffers of pH range 1.4–9.8. In cyclic voltammetry (CV) more than one oxidation peak was noticed in the acidic pH range and a single oxidation peak was observed in the neutral and alkaline pH range. The kinetics of decay of the UV-absorbing intermediate generated during electrooxidation has been studied at different pH and the decay occurred in a pseudo-first-order reaction. At pH 3.0, the electrooxidation products were characterized as alloxan-N^1-oxide, urea and alloxan in a 6e, $6H^+$ process. However, at pH 7.0, the number of electrons involved in the oxidation was found to be ~ 2.7 per mole and a dihydroxytrimer has been characterized as the major product. A detailed interpretation of the redox mechanism for the formation of the products has also been suggested.

Introduction

The oxidative transformation of purines into their *N*-oxide derivatives which are potent oncogenic agents introduces the possibility that such derivatives play an important role in various biological and clinical processes.[1–3] The presence of the *N*-oxide group in purines has been found to induce antibiotic activity.[4] Several purine *N*-oxides have been reviewed in relation to their oncogenic[5] and antitumor properties.[6] Heterocyclic aromatic *N*-oxides such as quinoxaline dioxides have been used in the treatment of tuberculosis, as anticancer agents and also as bioreductive drugs for the treatment of solid tumors.[7,8] The *N*-oxides of adenine and guanine have attracted considerable attention in the last few decades in view of the presence of these bases in DNA and RNA. The crystal and molecular structures of adenine N^1-oxide complexes have been reported.[9] Molecular orbital calculations for purine *N*-oxides have been carried out by Borbil *et al.*[10] to evaluate the stability of various *N*-oxides. Functioning of purine *N*-oxides as antimetabolites has also been reported in the literature.[11] Adenine N^1-oxide during the past few years has found utility in various organic and inorganic syntheses.[12–14]

Adenine N^1-oxide also acts as a competitive inhibitor of the change in shape induced in platelets by ADP.[15] In view of the importance of adenine N^1-oxide and its derivatives the polarographic and enzymic reduction of these compounds has been reported in the literature.[16,17] It was found that reduction of adenine N^1-oxide takes place *via* the formation of adenine. As oxidation reactions have been found to be of significance in biological systems,[18,19] it was considered interesting to study the electrooxidation of *N*-oxides. The presence of the *N*-oxide function introduces some profound differences from the parent purines in the behavior of both ring system and substituents. The objective of the present work is to study the electrooxidation of adenine N^1-oxide with the expectation that the results will provide deep insights into its redox chemistry. As electrochemical studies coupled with spectral techniques have been found useful in probing the oxidation chemistry of biologically significant molecules,[20] spectral changes during the electrooxidation and the kinetics of decay of the UV-absorbing intermediate were also monitored.

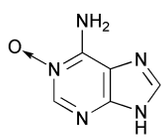

I

Experimental

Materials

Adenine N^1-oxide (**I**) monohydrate was obtained from Lancaster Synthesis, UK and was used as received. All other chemicals used were of analytical grade. A Cypress computer controlled electroanalytical system, model CS-1090, was used to carry out linear and cyclic sweep voltammetric studies. Phosphate buffers of ionic strength 1.0 M were prepared according to the method of Christian and Purdy.[21] A Century digital pH-meter, model CP-901-P, after due standardization was used to measure the pH of the buffer solutions. All potentials are reported with reference to the Ag/AgCl electrode at an ambient temperature of 20 ± 2 °C. Controlled potential electrolysis was carried out in a single compartment cell equipped with a three-electrode system using a pyrolytic graphite plate (6 × 1.5 cm^2) as working electrode, a cylindrical platinum gauge (1.5 × 5 cm^2) as auxiliary electrode and an Ag/AgCl electrode as reference electrode. Coulometric studies were carried out at a desired pH using a BAS CV-50W potentiostat.

The pyrolytic graphite electrode (PGE) (~ 4 mm^2) was prepared in the laboratory by the reported method.[22] After each voltammogram, polishing of the working electrode on a 600 grit metallographic disc was carried out to renew the PGE surface. The surface was then washed with a jet of distilled water and touched onto soft tissue paper gently. This procedure resulted in a significantly new surface for each run and showed a variation of ±10% in peak currents in repeated runs. Hence, for determining peak current values an average of at least three runs was taken.

Spectral studies during electrooxidation and kinetic studies of the UV-absorbing intermediate were carried out in 1 cm quartz cells using a Shimadzu UV-1601 PC spectrophotometer.

DOI: 10.1039/b204208h

Lyophilization of the electrolyzed solution was carried out using a Herysun lyophilizer. FT-IR spectra were recorded on a Perkin Elmer 1600 series FT-IR spectrophotometer using KBr pellets. The ^{1}H NMR spectrum of the product was recorded in d_6-DMSO on a DRX-300 spectrophotometer and its mass spectra were recorded using a JEOL SX 102/DA-6000 instrument. Thin layer chromatography was carried out using glass plates coated with silica gel-G obtained from Central Drug House, New Delhi.

Procedures

A stock solution (1 mM) of compound **I** was prepared in double distilled water. Solutions were prepared by mixing 2 ml of stock solution and 2 ml of phosphate buffer of desired pH. The solutions were deaerated by passing a stream of nitrogen gas for 10–12 min through them before recording the voltammograms. The progress of electrolysis was monitored by recording spectral changes at different time intervals. For this purpose, a potential 100 mV more positive than the oxidation peak potential was applied. The value of n, the number of electrons involved in oxidation, was determined by monitoring the exponential decay of the current–time curve as reported by Lingane.[23]

Spectral changes during electrolysis were monitored by transferring 2–3 ml of the electrolyzed solution into a quartz cell and recording the spectrum in the range 200–350 nm. When absorbance at λ_{max} reduced to about 50%, electrolysis was turned off by opening the circuit and spectral changes were monitored at different time intervals. The change in absorbance with time indicates that a UV/Vis absorbing intermediate is generated during oxidation. The kinetics of decay of the UV/Vis absorbing intermediate was also monitored by recording the change in absorbance with time at selected wavelengths. The values of rate constant k were calculated from the linear log $(A - A_\infty)$ *versus* time plots. For the identification of oxidation products, about 15–20 mg of compound **I** were exhaustively electrolyzed at a large PGE plate (6 × 1.5 cm^2) in the buffer of desired pH at a potential 100 mV more positive than the oxidation peak potential. The progress of electrolysis was monitored by recording cyclic voltammograms at different time intervals. When the oxidation peak had completely disappeared, the electrolyzed solution was removed from the cell, filtered using Whatman filter paper 42 and lyophilized. The colorless lyophilized material obtained at pH 6.9 was treated with methanol (2 × 5 ml). The concentrated methanolic extract obtained exhibited a single spot in TLC (R_f ~ 0.68; 80 : 20 methanol–H_2O). This material was further characterized using IR, ^{1}H NMR and mass spectra. At pH 2.6, however, the filtrate was lyophilized, freeze dried and then dissolved in 2 ml of H_2O. It was then passed through a glass column packed with Sephadex G-10 resin (Sigma, bead size 40–120 μ) using doubly distilled water as an eluent at a flow rate of 0.8 ml min^{-1}. The first peak P_1 in gel-permeation chromatography was found to contain phosphate as identified by a qualitative test of the yellow precipitate, with $(NH_4)_2MoO_4$. The remaining phosphate free fractions were collected separately and again lyophilized to obtain pure material. The dried materials obtained were characterized using IR, mp, ^{1}H NMR and mass spectra.

Results and discussion

Voltammetric studies

Linear sweep voltammetric studies of adenine N^1-oxide at a sweep rate of 20 mV s^{-1} exhibited an oxidation peak I_a in the entire pH range 1.4–9.8, when the sweep was initiated in the positive direction. At pH ≤ 4.0, two additional peaks, II_a and III_a, were observed at more positive potentials than peak I_a respectively. However, peaks II_a and III_a were ill defined and noticed as a bump, and at pH > 4.0 they merged with the background. Peak I_a, on the other hand, was well-defined and clearly noticed in the entire pH range. The peak potentials of peaks I_a, II_a and III_a were dependent on pH and shifted to less positive potentials with increase in pH. The E_p *versus* pH plots were linear for all the three peaks as shown in Fig. 1 and the

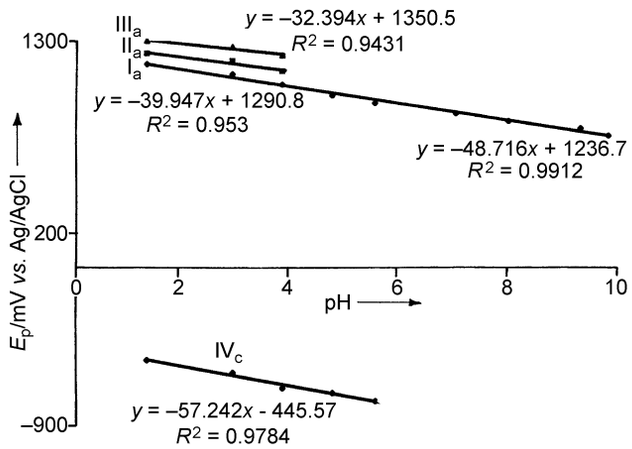

Fig. 1 Dependence of peak potential (E_p) on pH for the voltammetric oxidation and reduction peaks of 0.5 mM adenine N^1-oxide at PGE.

dependence of E_p on pH using linear regression analysis can be expressed by eqns. (1) to (3) having correlation coefficients 0.991, 0.953, 0.943, respectively.

$$E_p\ (I_a)\ [\text{pH } 1.4\text{–}9.8] = [1236.7\text{–}48.72\ \text{pH}]\ \text{mV } \textit{vs.}\ \text{Ag/AgCl} \quad (1)$$

$$E_p\ (II_a)\ [\text{pH } 1.4\text{–}4.0] = [1290.8\text{–}39.95\ \text{pH}]\ \text{mV } \textit{vs.}\ \text{Ag/AgCl} \quad (2)$$

$$E_p\ (III_a)\ [\text{pH } 1.4\text{–}4.0] = [1350.5\text{–}32.39\ \text{pH}]\ \text{mV } \textit{vs.}\ \text{Ag/AgCl} \quad (3)$$

Cyclic sweep voltammetry of compound **I** at a sweep rate of 100 mV s^{-1} exhibited an oxidation peak I_a in the entire pH range (1.4–9.8) when the sweep was initiated in the positive direction. Peaks II_a and III_a were noticed up to pH 4.0 and merged with the background at pH > 4.0. When reverse sweep was applied a reduction peak IV_c was observed in the pH range 1.4–5.6. On further reversal of the sweep towards the positive direction, no new anodic peak was noticed. Typical cyclic voltammograms of 0.5 mM solution of compound **I** at PGE at pH 2.6 and pH 6.9 are shown in Fig. 2, which clearly depicts the oxidation and subsequent reduction of the species generated during voltammetric studies. The peak potential of the cathodic peak IV_c was also dependent on pH and shifted to more negative potentials with increase in pH (Fig. 1). The dependence of E_p on pH for this reduction peak can be represented by eqn. (4) having correlation coefficient ~ 0.978.

$$E_p\ (IV_c)\ [\text{pH } 1.4\text{–}5.6] = [-445.6\text{–}57.24\ \text{pH}]\ \text{mV } \textit{vs.}\ \text{Ag/AgCl} \quad (4)$$

The peak current for peak I_a was found to increase with an increase in concentration of compound **I** in the range 0.1 to 1.5 mM. The graph plotted between i_p and concentration from data generated during CV studies was linear (Fig. 3) having correlation coefficient ~ 0.996. This behavior indicated that compound **I** could be safely estimated in the concentration range 0.1 to 1.5 mM at PGE. The effect of sweep rate on the peak current function of peak I_a was also studied in the range 20 to 1000 mV s^{-1} at pH 6.9. The peak current of peak I_a was found to increase with an increase in sweep rate. The peak I_a showed a tendency to merge with the background at a sweep rate > 500 mV s^{-1}. The plots of $i_p/\sqrt{v}$ *versus* log v (Fig. 4) indicated that the peak current function increased with increase in logarithm of sweep rate. This behavior indicated the

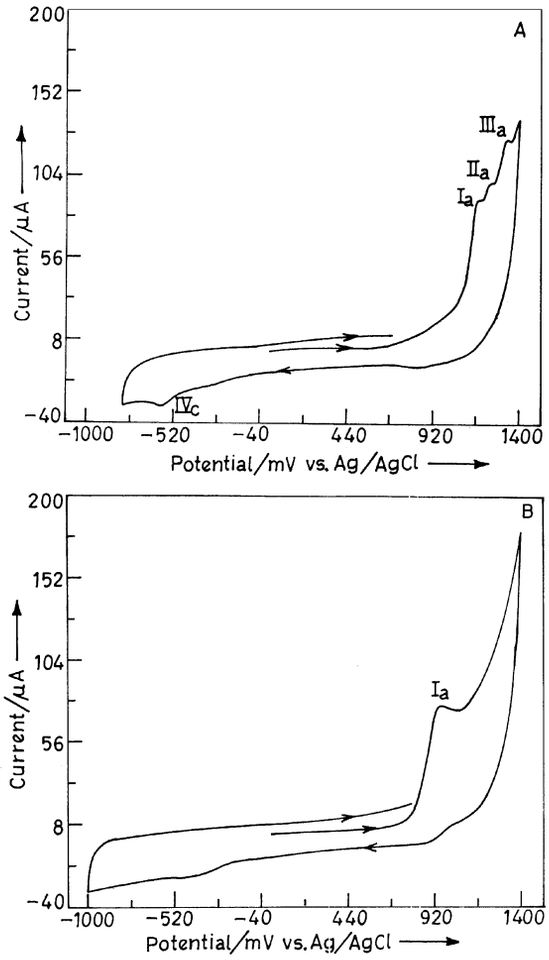

Fig. 2 Typical cyclic voltammograms of 0.5 mM adenine N^1-oxide at PGE in phosphate buffers of pH (A) 2.6 and (B) 6.9. Sweep rate 100 mV s^{-1}.

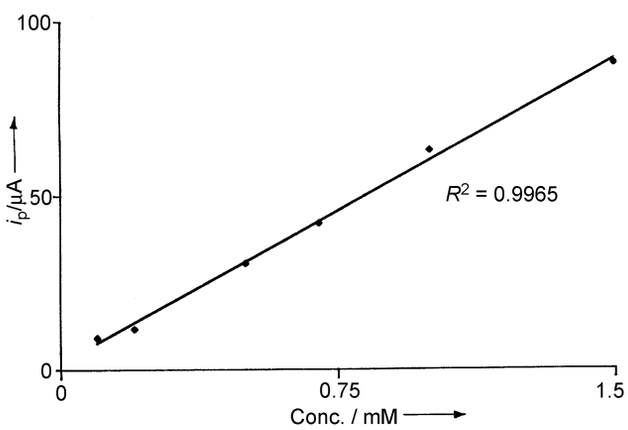

Fig. 3 Dependence of peak current (i_p) of peak I_a on concentration of adenine N^1-oxide at PGE at pH 6.9. Sweep rate 100 mV s^{-1}.

strong adsorption of the reactant at the surface of PGE.[24,25] Reduction peak IV_c was relatively small in the entire pH range and presumably influenced by the adsorption phenomenon.

Controlled potential electrolysis of compound **I** was performed at different pH in phosphate buffers. As the E_p values of peaks I_a, II_a and III_a were very close in the pH range 1.4–4.0, the value of n was determined at peak III_a potential whereas at pH ≥ 6.9, the value of n was determined at peak I_a potentials. The number of electrons n involved in electro-oxidation was determined by graphical integration of the current–time curve. The plot of i_p *versus* time was exponential in nature (Fig. 5). The value of n was found to be 5.7 ± 0.2 at pH 2.6 whereas at pH ≥ 6.9 the value was 2.6 ± 0.2. The

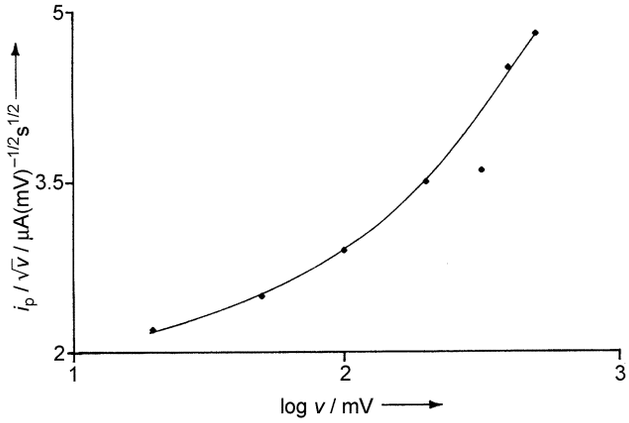

Fig. 4 Dependence of $i_p/\sqrt{v}$ on log v for peak I_a of 0.5 mM adenine N^1-oxide at pH 6.9.

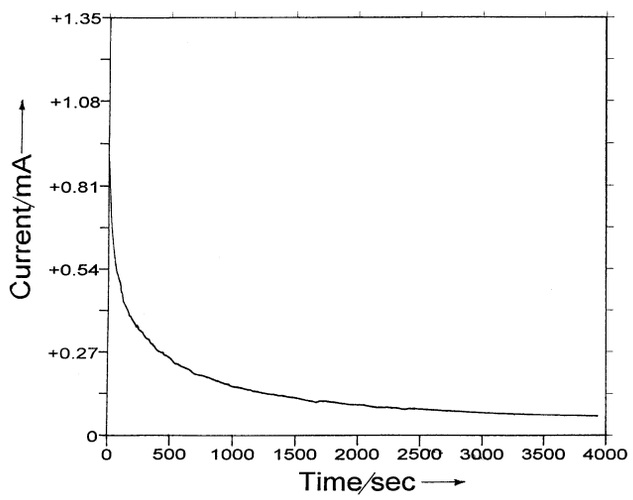

Fig. 5 Plot of current *versus* time observed for 0.5 mM adenine N^1-oxide in phosphate buffer at pH 2.6.

different n values in acidic and neutral or alkaline media indicate that the oxidation in acidic medium proceeds by a mechanism different from that in neutral and alkaline pH.

Spectral studies

The UV spectra of 0.1 mM solution of adenine N^1-oxide were recorded at different pH values in the range 1.4–9.8. At pH 2.6, two well-defined λ_{max} at 230 and 260 nm were clearly observed along with a shoulder at around 215 nm in 0.05 mM solution of adenine N^1-oxide. Curve 1 in Fig. 6 is the initial spectrum of compound **I** just before electrooxidation. Upon application of potential, 1.28 V, the absorbance first decreased in the region 200–280 nm whereas an increase in absorbance was observed in the region 280–350 nm (curve 2) and then a systematic increase in absorbance was noticed (curves 3–9). Curve 9 was recorded after 2 h and showed a significant increase in absorbance and three λ_{max} at 210, 227 and 256 nm were noticed. Thus, the shoulder at 215 nm of compound **I** was converted to well-defined λ_{max} at 210 nm and the maximum at 260 nm was shifted to shorter wavelength (256 nm).

On the other hand in the pH range 6.9–9.8, compound **I** exhibited two well-defined λ_{max} at 230 and 260 nm and a shoulder at 203 nm. Curve 1 in Fig. 7 presents the UV spectrum of adenine N^1-oxide at pH 6.9 just before electrooxidation. Upon application of a potential 100 mV more positive than peak I_a at PGE the absorbance in the regions 200–215 and 300–350 nm increased systematically (curves 2 to 9). However, in the region 215–300 nm the absorbance systematically decreased. Two clear isosbestic points were observed at 215 and 290 nm. Curve 9 was recorded after 2 h of electrolysis.

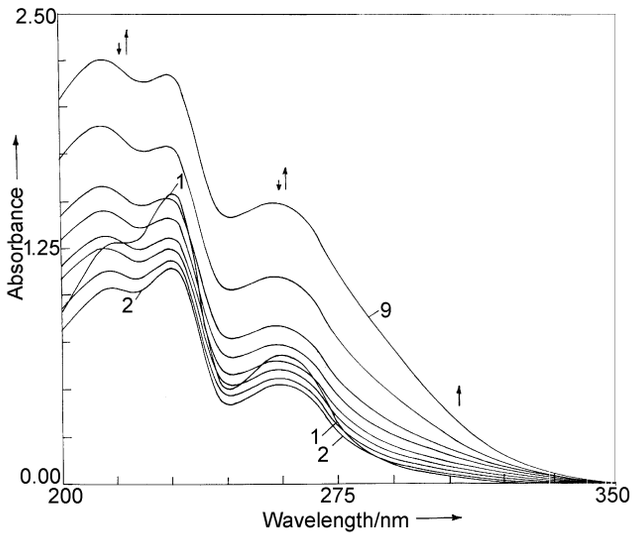

Fig. 6 Spectral changes observed during electrooxidation of 0.05 mM adenine N^1-oxide at pH 2.6; potential 1.28 V *vs.* Ag/AgCl. Curves were recorded at intervals of (1) 0; (2) 5; (3) 5; (4) 10; (5) 10; (6) 15; (7) 15; (8) 30; (9) 45 min of electrolysis.

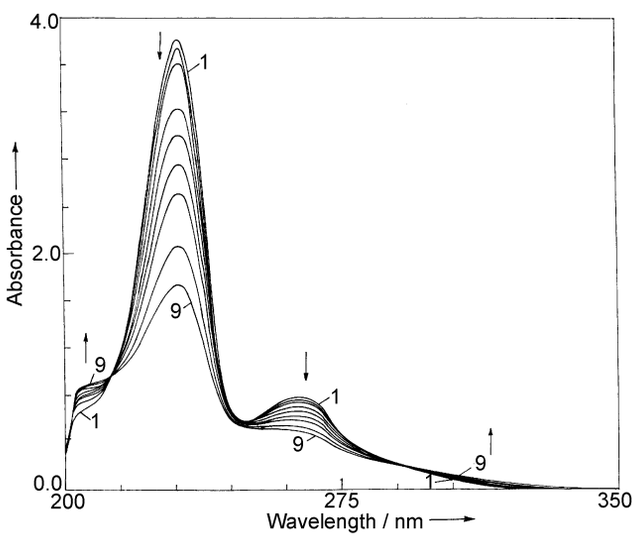

Fig. 7 Spectral changes observed during electrooxidation of 0.51 mg of adenine N^1-oxide at pH 6.9; potential 1.06 V *vs.* Ag/AgCl. Curves were recorded at intervals of (1) 0; (2) 5; (3) 5; (4) 10; (5) 10; (6) 15; (7) 15; (8) 30; (9) 45 min of electrolysis. The corresponding coulombs passed are (1) 0; (2) 0.075; (3) 0.093; (4) 0.099; (5) 0.135; (6) 0.180; (7) 0.243; (8) 0.567 and (9) 0.747.

In a separate experiment the applied potential was switched to zero volt when absorbance at λ_{max} reduced to 50% and the spectral changes were monitored. It was found that the absorbance in the region 250–300 nm systematically decreased in the entire pH range. Hence, it was concluded that a UV-absorbing intermediate is generated during electrooxidation. The kinetics of decomposition of the UV-absorbing intermediate was monitored at 260 and 290 nm by recording changes in absorbance with time at selected wavelengths. The resulting absorbance *versus* time profiles showed an exponential decay as presented in Fig. 8. The values of the pseudo first order rate constant (k) were determined at different pH, using log ($A - A_\infty$) *versus* time plots (inset, Fig. 8) and were found to be in the range (0.23–0.69) × 10^{-3} s^{-1}. The values of k calculated at different pH and wavelengths are presented in Table 1. An examination of Table 1 clearly indicates that the decay of the UV-absorbing intermediate is an acid–base catalyzed reaction, as the values of k did not change significantly with change in pH.

Table 1 Rate constants observed for the decay of the UV/Vis absorbing intermediate of adenine N^1-oxide at different pH at PGE

pH	λ_{max}/nm	$k/10^{-3}$ s^{-1}
2.6	260	0.46
	290	0.23
4.8	260	0.69
	290	0.46
6.9	260	0.69
	290	0.46
9.4	260	0.46
	290	0.69

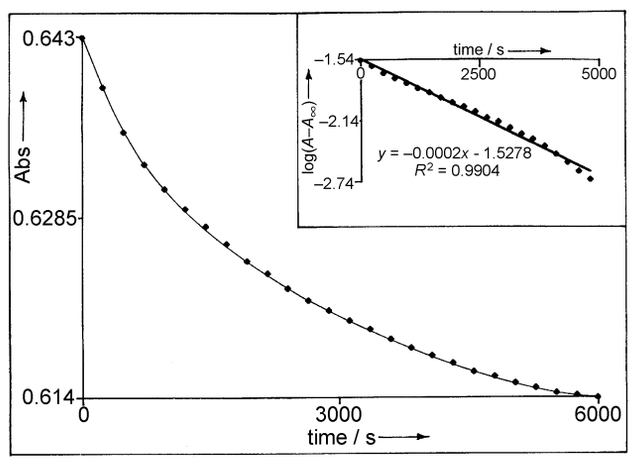

Fig. 8 Plot of absorbance *versus* time and log ($A - A_\infty$) *versus* time (inset) plot measured at 260 nm for the decay of the UV-absorbing intermediate generated during electrooxidation of 0.1 mM adenine N^1-oxide at PGE, at pH 6.9.

Product characterization

The ultimate products of electrooxidation of adenine N^1-oxide were isolated and characterized at pH 2.6 and 6.9. TLC studies of the freeze-dried material exhibited three spots at pH 2.6 and a single spot at pH 6.9. At pH 2.6, the products were separated by gel permeation chromatography (see Experimental) and the plot of absorbance *versus* volume exhibited three peaks. The first peak P_1 (150–210 ml) was found to contain phosphate and hence discarded. The lyophilized material obtained from the volume under second peak P_2 between 210–300 ml gave a single spot in TLC (R_f ~ 0.43) and had a mp of 240 °C. A clear molecular ion peak was obtained at m/z = 157 (90%) in the mass spectrum of this material. The other high mass peaks observed in the fragmentation pattern were at 179 (69.0%), 198 (7.1%), 217 (7.8%), 235 (30%), 277 (18.1%), 299 (15.3%), 315 (12.8%), 335 (60.2%) and 355 (29.7%). The material also gave prominent peaks in the FT-IR spectrum at 3330, 1290 (secondary >NH), 1680 (cyclic >C=O), 1510 (N⟶O), 1392 and 720 (C–N and C–C) cm^{-1}, clearly indicating that the N⟶O linkage is present in the material. The ^{1}H NMR spectrum of the product exhibited only one signal at δ = 8.1 (s, 1 H), which corresponds to the proton of NH present in the pyrimidine ring and hence it was concluded that the product was alloxan N^1-oxide which was further confirmed by recording its UV spectrum. It was noticed that the UV spectrum (λ_{max} ~ 230 and 260 nm) was similar to that of authentic alloxan N^1-oxide. The formation of alloxan N^1-oxide suggests that the rupture of the imidazole ring of adenine N^1-oxide occurs at pH 2.6 and hence the other product should be urea, which could not be identified. Urea, owing to its low molecular weight, has been found to elute with phosphate in gel-permeation chromatography. This fact was confirmed by passing a small quantity of urea (~ 1 mg) through the Sephadex G-10 column under identical conditions. It was found that urea elutes between 160–190 ml.

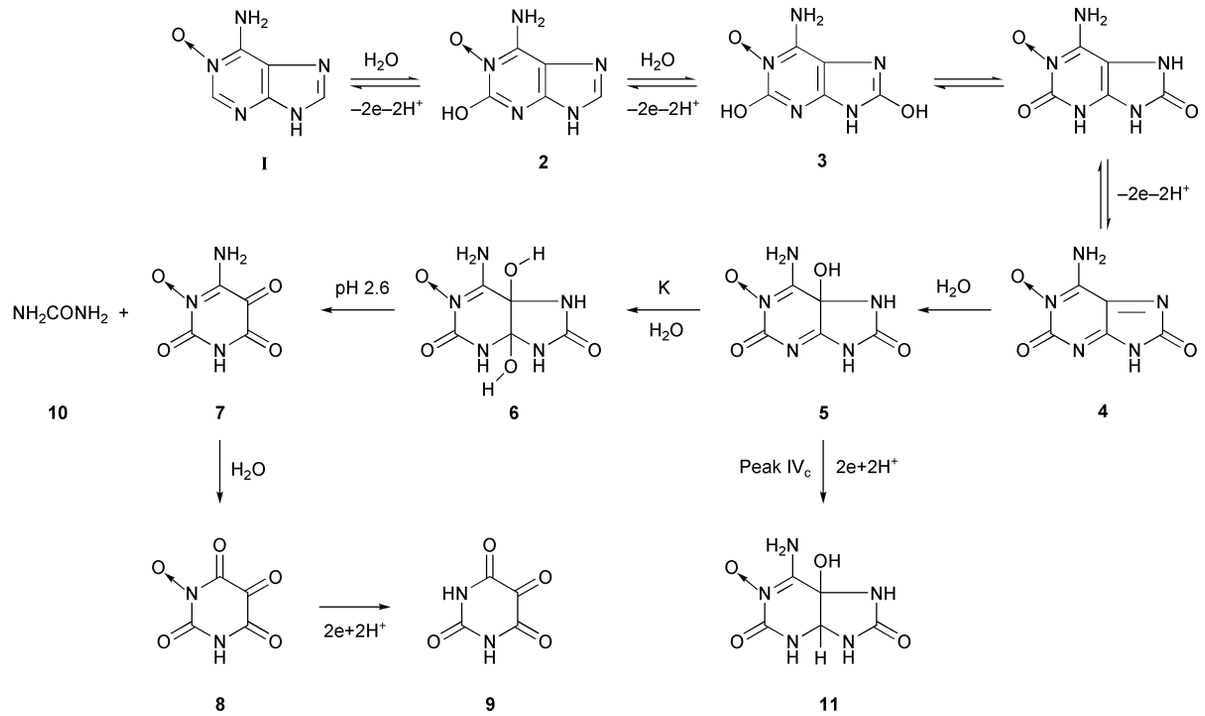

Scheme 1 Proposed mechanism for the electrooxidation of adenine N^1-oxide at pH 2.6.

The colorless freeze-dried material under peak P_3 (300–340 ml) exhibited a single spot in TLC (R_f ~ 0.4) and had a mp of 245 °C. The colorless material exhibited strong IR bands at 1260 (N–H), 1640 (cyclic >C=O), 1160, 708 (C–N and C–C) cm^{-1} and λ_{max} at ~ 260 nm. The ^1H NMR spectrum exhibited sharp peaks at δ 7.46 (s, NH) and 7.24 (s, NH) and a clear molecular ion peak at m/z = 160 (35%) confirmed the product as alloxan monohydrate (**9**) as shown in Scheme 1.

At pH 6.9 the concentrated methanolic extract of the lyophilized material exhibited a single spot in TLC (R_f ~ 0.68). Prominent peaks obtained in the FT-IR spectrum were at 3000, 750 (aromatic C–H), 3500 (–OH), 3374 (secondary >NH), 1720 (C=N), 1650 (C=C), 1480 (N⟶O), 1280 (C–NH–C) cm^{-1}. The mass spectrum of the material exhibited a clear molecular ion peak at m/z = 482 (17.8%, M + 1) and thus suggested the molar mass of the material as 481. Other high mass peaks observed in the fragmentation pattern were at 234 (18.0%), 254 (66.2%), 289 (19.0%), 307 (20.5%), 329 (84.3%), 353 (14.1%), 413 (27.8%), 443 (16.7%) and 462 (29.1%). The molar mass of 481 of the product indicated it to be a trimer. The ^1H NMR spectrum of the product exhibited signals at δ 8.35 (s, 2H), 8.23 (s, 2H), which belong to two NH_2 groups present in the molecule. The signals present at δ 8.18 (s, 1H), 8.10 (s, 2H), 7.97 (s, 1H), 7.28 (s, 1H) and 7.20 (s, 1H) belong to various NH and OH groups (total 6, 4 NH + 2 OH) present in the molecule. At this stage the position of one aromatic proton could not be established with certainty, however, a comparison of the δ value with adenine (δ = 6.5) indicates the possibility of a signal at δ 7.12 due to the aromatic proton. The range of aromatic protons has been reported in the range δ 6.5 to 7.2. The downfield shift of 0.62 in the position of the aromatic proton could be due to various bulkier substituents present at positions 6 and 8 of the middle ring of trimer **VI**. On integration the total number of protons was found to be 11.

The molar mass of 481 suggests that at least three units of adenine N^1-oxide combine together to form a trimer. The presence of a strong band at 1280 cm^{-1} in the FT-IR spectrum suggests the presence of a C–NH–C linkage in the trimer **VI**. Such a linkage can be obtained by the combination of two rings at 8 and 6′ positions through free radicals generated in primary electrode reactions ($\mathbf{II}_a$ and $\mathbf{II}_b$). The ^1H NMR spectrum indicated the presence of two NH_2 groups and four NH groups, with no proton at adjacent carbons because in such an event, the signal would have been observed as a multiplet. Thus, out of the three rings present in the trimer, two are attached through 8 and 6′ positions. The attachment of the third ring to dimer $\mathbf{III}_b$ can occur in two different ways. First, $\mathbf{III}_b$ can combine with $\mathbf{II}_a$ *via* positions 8′–6″ to give a C–NH–C linkage. A second possibility is the attachment of $\mathbf{II}_b$ to dimer $\mathbf{III}_b$ *via* 8′–8″ positions leading to a C–C linkage. Out of the two possibilities the first possibility was excluded on the basis of two NH_2 signals in the ^1H NMR spectrum of the trimer. If attachment of $\mathbf{II}_a$ had occurred only one NMR signal corresponding to NH_2 would be expected. Thus, it was concluded that for the third ring, $\mathbf{II}_b$ attached to dimer $\mathbf{III}_b$ to give trimer **IV** as shown in Scheme 2. The presence of –OH groups indicated by a sharp FT-IR band at around 3500 cm^{-1} was also confirmed by signals at δ 7.28 and δ 7.20 in the ^1H NMR spectrum of the product. Likely positions for attachment of –OH in hydroxylated trimer **VI** are 2, 2′ and 2″. However, positions 2 and 2″ seem to be more favorable for hydroxylation in view of steric hindrance at position 2′ because of the bulkier group present at position 6′. The UV-spectrum of hydroxylated trimer **VI** exhibited λ_{max} at 230 and 260 nm as shown in Fig. 9.

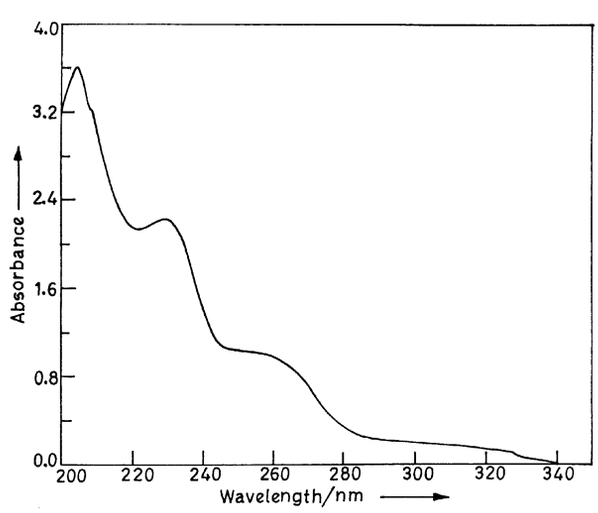

Fig. 9 UV spectrum of ~ 0.01 mM of product **VI** at pH 6.9.

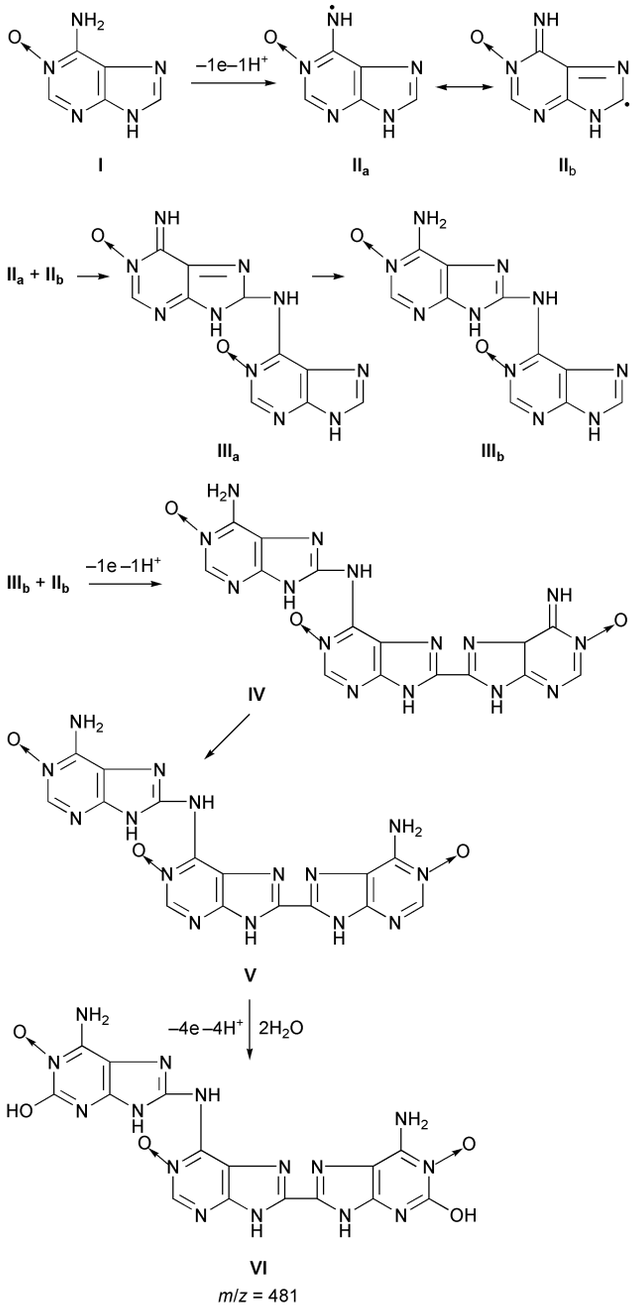

Scheme 2 Proposed mechanism for the electrooxidation of adenine N^1-oxide at pH 6.9.

Redox mechanism

The results obtained above indicate that electrooxidation of adenine N^1-oxide occurs by a mechanism involving a 6e, $6H^+$ process in the acidic pH range to form alloxan and alloxan-N^1-oxide as the major products, whereas in the neutral and alkaline pH range a hydroxy trimer has been characterized. At pH 2.6, the initial 2e, $2H^+$ oxidation of adenine N^1-oxide (**1**) can form either 2-hydroxy- or 8-hydroxyadenine N^1-oxide. However on the basis of studies on the oxidation of adenine reported in the literature,[26] it seems reasonable to conclude that the first 2e, $2H^+$ oxidation leads to 2-hydroxyadenine N^1-oxide (**2**) which on further 2e, $2H^+$ oxidation forms 2,8-dihydroxyadenine N^1-oxide (**3**). As oxidation of hydroxy purines occurs at less positive potentials in comparison to simple purines, it is expected that 2,8-dihydroxyadenine N^1-oxide (**3**) readily undergoes further oxidation in a 2e, $2H^+$ step to give the corresponding diimine (**4**). The increase in absorbance during spectral studies is most likely due to the formation of diimine **4**, which possesses a highly conjugated π-system and hence absorbs at longer wavelength. The formation of diimine and its short half life (~ 50 ms) have been well documented during electrooxidation of uric acid and other purines.[27,28] The dimines have been reported as highly unstable and therefore a water molecule rapidly attacks to form imine alcohol **5**. The attack of a second water molecule on **5** will be a slow process and leads to the formation of diol **6**. The k values observed in the spectral studies represent the decomposition of imine alcohol to diol **6** in a pseudo first-order reaction. The cleavage of the imidazole ring then occurs to give urea (**10**) and 6-amino-2,4,5-trioxopyrimidine-N^1-oxide (**7**). The conversion of compound **7** to **8** requires protonation of the amino group. The deamination followed by hydrolysis gives alloxan-N^1-oxide (**8**) and ammonia as the final products as shown in Scheme 1. The formation of alloxan (**9**) in controlled potential electrolysis appears to be from the reduction of alloxan-N^1-oxide in a 2e, $2H^+$ process. The stability of adenine N^1-oxide[29] has been well reported in aqueous and alkaline media whereas its conversion to adenine has been reported in acidic medium. Thus, it seems reasonable to conclude that the formation of alloxan occurs due to the hydrolysis of alloxan-N^1-oxide.

In contrast to pH 2.6, only one product was formed from the oxidation of adenine N^1-oxide at pH 6.9. The coulometric determination indicated that 2.6 ± 0.2 electrons per mole were involved. The number of F/mole, which can be deduced from Scheme 2, is 2.7. As the experimental value is 2.6, it is interesting to point out that the two values agree reasonably with each other. Thus initial one-electron oxidation of adenine N^1-oxide (**I**) gives a free radical species which can exhibit several resonating forms as shown in Scheme 2. Two free radicals $\mathbf{II}_a$ and $\mathbf{II}_b$ can easily combine to form a dimer ($\mathbf{III}_a$) in which the two moieties are linked to each other by –NH– linkage. The dimer $\mathbf{III}_a$ will aromatize to give the more stable dimer $\mathbf{III}_b$. The 1e, $1H^+$ oxidation of $\mathbf{III}_b$ gives a free radical at position 8′, which combines with $\mathbf{II}_b$ to give a trimer **IV**. Position 8′ has been found to be highly susceptible to oxidation in the dimers of a variety of purines and their derivatives.[30] Thus, the product of oxidation of adenine N^1-oxide in neutral and alkaline medium appears to be a trimer (**IV**) which aromatizes to give stable trimer **V**. The ultimate product, however, is a dihydroxytrimer **VI** formed on further 4e, $4H^+$ oxidation of trimer **V**. The trimer **VI** has a molar mass of m/z = 481 having two –OH groups as shown in Scheme 2.

The appearance of peak IV_c in the CV of adenine N^1-oxide in the pH range 2.6–5.6 appears to be due to the reduction of the imine alcohol **5** to form a dihydro species (**11**). Reduction of imine alcohols to give dihydro species has been well reported in the literature.[31]

The present studies clearly indicate that oxidation of adenine N^1-oxide is much more complicated than that of the corresponding purine adenine. The formation of oligomers during oxidation of adenine N^1-oxide may be one of the reasons for making it oncogenic in nature. The formation of the observed products is always possible by more than one route, however, the proposed mechanism explains all the observed voltammetric, coulometric and spectral data. The toxicity evaluation of the hydroxylated trimer **VI** is under investigation and will be reported later.

Acknowledgements

A. Sangal is grateful to the Department of Science and Technology, New Delhi for a Junior Research Fellowship. Thanks are also due to the Director, CDRI, Lucknow for providing mass and ^{1}H NMR spectra of the samples.

References

1 T. Fujii, K. Ogawa, T. Itaya, T. Date, J. Inagaki and F. Nohara, *Chem. Pharm. Bull.*, 1995, **43**, 408.

2 K. Ogawa, M. Nishii, F. Nohara, T. Saito, T. Itaya and T. Fujii, *Chem. Pharm. Bull.*, 1992, **40**, 612.
3 G. B. Brown, *Prog. Nucleic Acid Res. Mol. Biol.*, 1968, **8**, 209.
4 F. Nohara, M. Nishii, K. Ogawa, K. Isono, M. Ubukata, T. Fujii, T. Itaya and T. Saito, *Tetrahedron Lett.*, 1987, **28**, 1287.
5 K. Ogawa, M. Nishii, J. Inagaki, F. Nohara, T. Saito, T. Itaya and T. Fujii, *Chem. Pharm. Bull.*, 1992, **40**, 343.
6 K. Sugiura, *Cancer Chemother. Rep. 2*, 1968, **1**, 383.
7 Y. Sainz, M. E. Montaya, F. J. M. Crespo, M. A. Ortego, A. Lopez de Cerain and A. Monge, *Arzneim.-Forsch.*, 1999, **49.I**, 55.
8 H. U. G. Muhtasib, M. J. Haddadin, D. N. Rahhai and I. H. Younes, *Oncol. Rep.*, 2001, **8**, 679.
9 P. Prusiner and M. Sundaralingam, *Acta Crystallogr., Sect. B*, 1972, **28**, 2142.
10 M. Borbil, R. Nutiu, M. Mracec and Z. Simon, *Rev. Roum. Biochim.*, 1978, **15**, 3.
11 G. B. Brown, D. A. Clarke, J. J. Biesele, L. Kaplan and M. A. Stevens, *J. Biol. Chem.*, 1958, **233**, 1509.
12 T. Fujii, K. Ogawa, T. Saito, T. Itaya, T. Date and K. Okamura, *Chem. Pharm. Bull.*, 1995, **43**, 321.
13 M. Kezdi, H. Mantsch, L. Muresan, C. Tarmura and O. Barzu, *FEBS Lett.*, 1973, **33**, 33.
14 C. M. Mikulski, R. De Prince, B. T. Thu, F. J. Iaconianni, L. L. Ptylewski, A. N. Speca and N. M. Karayannis, *Inorg. Chim. Acta*, 1981, **56**, 163.
15 J. J. Sixma, H. Holmsen and A. C. M. Trieschnigg, *Biochim. Biophys. Acta*, 1973, **298**, 460.
16 C. R. Warner and P. J. Elving, *U.S. At. Energy Comm.* C00–1148–95, 1965, p. 18.
17 G. Stoehrer and G. B. Brown, *J. Biol. Chem.*, 1969, **244**, 2498.
18 B. Clement and T. Kunze, *Arch. Pharm.*, 1993, **326**, 125.
19 T. Itaya, K. Ogawa, Y. Takada and T. Fujii, *Chem. Pharm. Bull.*, 1996, **44**, 967.
20 K. Rajeshwar, R. O. Lezna and N. R. de Tacconi, *Anal. Chem.*, 1992, **64**, 429A.
21 G. D. Christian and W. C. Purdy, *J. Electroanal. Chem.*, 1982, **3**, 363.
22 F. J. Miller and H. E. Zittel, *Anal. Chem.*, 1963, **35**, 1866.
23 J. J. Lingane, *Electroanalytical Chemistry*, 2nd edn., Wiley, New York, 1966, p. 222.
24 R. S. Wopschall and I. Shain, *Anal. Chem.*, 1967, **39**, 1514.
25 R. S. Nicholson and I. Shain, *Anal. Chem.*, 1964, **36**, 706.
26 R. N. Goyal, A. Kumar and A. Mittal, *J. Chem. Soc., Perkin Trans. 2*, 1991, 1369.
27 R. N. Goyal, A. B. Toth and G. Dryhurst, *J. Electroanal. Chem.*, 1982, **133**, 282.
28 E. Teresa, A. Peterson and A. B. Toth, *J. Electroanal. Chem.*, 1988, **239**, 1612.
29 M. A. Stevens, D. I. Magrath, H. W. Smith and G. B. Brown, *J. Am. Chem. Soc.*, 1958, **80**, 2755.
30 P. Subramanian and G. Dryhurst, *J. Electroanal. Chem.*, 1987, **224**, 137.
31 R. N. Goyal and N. K. Singhal, *Indian J. Chem., Sect. A*, 1999, **38**, 49.